Surface Brillouin-scattering spectroscopy of media with nonuniform acousto-optic properties

R. Caporali, C. E. Bottani,* and G. Ghislotti*

Dipartimento di Ingegneria Nucleare del Politecnico di Milano, Via Ponzio, 34/3 20133 Milano, Italy

(Received 1 June 1995)

We present a theoretical tool to compute the Brillouin-scattering cross section for shear horizontal (SH) surface phonons in an inhomogeneous medium with any type of depth profiles of elastic, dielectric, and elasto-optic properties. The acoustic eigenmodes are found by means of numerical solution of a self-adjoint Liouville equation with the boundary conditions of a finite slab. Both discrete and continuous phonon spectra are studied. The layer projected phonon density of states for the SH polarization is used to analyze the surface character of the modes. Also, the transmitted (zeroth-order) electromagnetic field and the reflection coefficient are obtained numerically solving Maxwell's equations. The scattered field is computed (in a way similar to that of the zeroth-order field) by first-order perturbation theory as a result of the smallness of the phonon excitations. The backscattering p-s Brillouin spectrum is obtained by summing the scattering intensity from individual acoustic modes over the density of phonon states at a generic incidence angle. As an example, we present the case of a Si/SiO$_2$ bilayer on a Si(001) substrate with sharp or smooth interfaces between silicon and silica. We think the method is promising in view of the application of surface Brillouin-scattering spectroscopy to real imperfect materials.

I. INTRODUCTION

The spectrum of long-wavelength surface acoustic phonons in opaque or semiopaque materials, mainly in the form of homogeneous media or of supported films, has been extensively investigated by means of Brillouin scattering of laser light. For a review see, e.g., Ref. 1.

Most of the studies have dealt with surface acoustic phonons polarized in the sagittal plane, defined by the surface phonon propagation wave vector, $\mathbf{q}_{||}$, and the surface normal. For this type of excitation, light scattering occurs through the surface ripple and the volume elasto-optic effect. So far, instead, the case of shear horizontal (SH) surface phonons, polarized parallel to the surface, has not received great attention. The main reason is the experimental difficulty of detecting this type of phonon peak in Brillouin spectra. Yet a great deal of acoustic and geophysical literature exists about shear horizontal surface elastic waves,[2] and the corresponding mathematical treatment is easier than that needed to treat saggital waves. Only recently two papers[3,4] have appeared treating the case of shear horizontal phonons in silicon on insulator structures (SOI) obtained by ion implantation of oxygen in silicon (SIMOX technology). These works showed and explained theoretically the existence and the dispersion properties of a surface mode localized in the buried silica layer characteristic of the SIMOX structures and of a pseudosurface mode nearly localized in the top silicon layer. At the present state of the art good SIMOX structures have rather sharp interfaces between silicon and silica, the transition region being of the order of a few nanometers. Sometimes, however, these structures present silicon inclusions in the silica layer and silica inclusions both in the top and substrate silicon, as can be seen by SIMS and TEM measurements.[5] Provided a local effective medium approximation is applicable,[6] depending on the acoustic and electromagnetic wavelengths and inclusion sizes and concentration, the real structure can be seen as one with diffuse (smooth) interfaces; see Fig. 1. Aside from this particular case we have in mind a much more general situation of variable composition materials where, at least at the mesoscopic level, the inhomogeneity of all relevant physical properties is one dimensional.[6]

The problem of computing the p-s Brillouin cross section for such media has been recently solved by Bottani and Caporali and presented in Ref. 7. Hereafter we give a more detailed account of our method with explicit expressions for the acoustic and electromagnetic fields and further examples of application.

The existing algorithms for computing Brillouin cross sections (p-p, p-s) in layered media assume that (a) all the physical properties are space independent in each layer; (b) the displacement vector field and the normal component stress of the tensor are continuous across the ideally sharp interfaces connecting all neighboring layers. Both Green function and mode-matching methods have been used to treat these problems always using the concept of partial plane-wave analysis for the acoustic and the electromagnetic fields in each layer. Here, we adopt a completely different but equivalent approach. We consider the whole medium as a thick slab with two free surfaces and depth-dependent physical properties in a limited subsurface region at one side. The inhomogeneous portion of the system is described giving the z profiles of all the physical coefficients. Photon absorption is normally assumed to make the transmitted field to vanish within a depth much smaller than the slab thickness, allowing one to consider semi-infinite the medium as far as the electromagnetic computation is concerned even though this is not a must to apply our method. The paper is organized as follows. We describe the theoretical tools needed to compute the following.

(i) The spectrum of surface SH phonons in the structure by means of a numerical solution of the self-adjoint Liouville equation governing the propagation of this kind of surface acoustic waves.

(ii) The fluctuating polarization vector field $\mathbf{P}_y$ produced
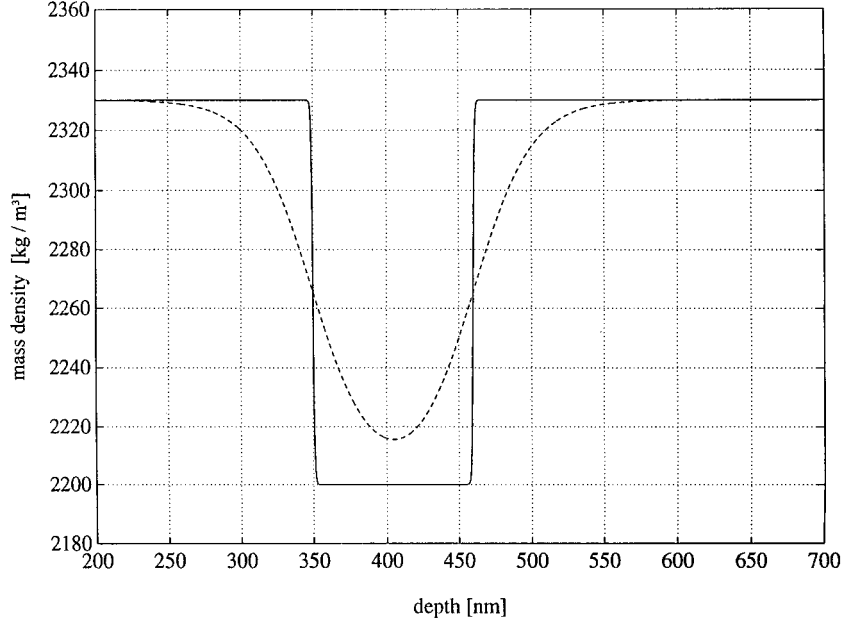
FIG. 1. Typical depth profile of the density $\rho(z)$ of two model SOI structures with different width δ. $\delta = 1$ nm (solid line), $\delta = 40$ nm (dashed line).

by thermal agitation through the elasto-optic coupling. The knolewdge of $\mathbf{P}_y$ required a numerical computation of the transmitted zeroth-order field in the medium.

(iii) the p-s Brillouin cross section. This implies solving the wave equation for the scattered electromagnetic field in the medium with a numerical method.

(iv) At last, the theoretical results are applied to the particular case of a model imperfect silicon on insulator structure with diffuse effective interfaces. The intensity, nature, and position of found peaks can be explained in terms of the layer projected phonon spectrum, the corresponding polarization vector fields, and the transmission properties of the medium.

II. LAYER-PROJECTED SHEAR HORIZONTAL ACOUSTIC PHONON SPECTRUM

The mechanical displacement vector field $\mathbf{u} = [u_i]$ produced by a thermal acoustic wave crossing the medium satisfies the equation[8]

$$\text{div}\boldsymbol{\Sigma} = \rho \frac{\partial^2 \mathbf{u}}{\partial t^2}, \tag{1}$$

where $\boldsymbol{\Sigma} = [\sigma_{ij}]$ is the stress tensor field and $\rho(z)$ the mass density depth profile.

We consider only shear horizontal (SH) surface acoustic waves (SAW's) propagating in a layered medium along any direction parallel to the $y = 0$ plane (which is both the sagittal and the scattering plane in our scheme) and, therefore, we deal only with the displacement field component u_y. Besides, we assume that the SH SAW's propagate along the x direction. We take into account only [100] and [110] propagation directions and (001) surfaces because, in these cases, sagittal motion is decoupled from the SH one. In particular, the wave equation for u_y, when the x axis corresponds to the

[100] direction, can be obtained from Eq. (1) and generalized Hooke's law for cubic media as[8]

$$\rho(z) \frac{\partial^2 u_y}{\partial t^2} = C_{44}(z) \frac{\partial^2 u_y}{\partial x^2} + \frac{\partial}{\partial z}\left[C_{44}(z) \frac{\partial u_y}{\partial z}\right], \tag{2}$$

where $C_{44}(z)$ is the depth profile of one of the three independent elastic moduli of the system. Instead of considering an ideal semi-infinite medium we treat here the case of a thick slab[9] with two free surfaces and depth-dependent physical properties in a limited region at one side. The inhomogeneous portion of the system is described giving the z profiles of the elastic coefficients, mass density, dielectric function, and elasto-optic coefficients.[6] Practically, any z dependence of the above properties is allowed. All the functions of z are required to become smoothly constant in the "bulk" portion of the system, i.e., the substrate.

As a consequence of the translational invariance of the system in the x direction parallel to the surface, we define the $(\omega, q_{||})$ Fourier component of the u_y SH displacement field, being the parallel wave vector $\mathbf{q}_{||} = q_{||}\hat{\mathbf{e}}_x$, as

$$u_y(\omega, q_{||}; x, z, t) = \xi(\omega, q_{||}) \phi_y(\omega, q_{||}, z)\exp[i(q_{||}x - \omega t)], \tag{3}$$

where $\xi(\omega, q_{||})$ is the normal coordinate of the SH phonon $(\omega, q_{||})$. If we introduce (3) in the wave equation (2) it results the self-adjoint Liouville equation[10]

$$\frac{d}{dz}\left[C_{44}(z) \frac{d\phi_y(\omega, q_{||}, z)}{dz}\right]$$
$$+ [\rho(z)\omega^2 - C_{44}(z)q_{||}^2]\phi_y(\omega, q_{||}, z) = 0, \tag{4}$$

where the mode z profiles $\phi_y(\omega, q_{||}, z)$ are the real eigenfunctions of Eq. 4 corresponding to the real eigenvalues $\omega^2 = \omega^2(q_{||})$, that is, the SH phonon eigenfrequencies. We can think that the $\phi_y(\omega, q_{||}, z)$'s correspond, in our con-

tinuum model, to the polarization unit vectors in lattice dynamics.[9] An analogous Liouville equation is obtained for the $\langle 110 \rangle$ case substituting $\frac{1}{2}[C_{11}(z) - C_{12}(z)]$ to $C_{44}(z)$ as the multiplying coefficient of $q_{||}^2$ in Eq. (4).

The normalization conditions are[10]

$$\int_0^h \rho(z) \phi_y^2(\omega, q_{||}, z) dz = 1, \qquad (5)$$

h being the overall slab thickness.

We assume stress-free boundary conditions at both $z = 0$ and $z = h$. This implies the vanishing of the z derivative of the mode profiles at these surfaces:

$$\left(\frac{d\phi_y(\omega, q_{||}, z)}{dz} \right)_{z=0} = \left(\frac{d\phi_y(\omega, q_{||}, z)}{dz} \right)_{z=h} = 0. \qquad (6)$$

Equations (4), (5) and (6) form a well-posed Sturm-Liouville eigenvalue problem.[10] Furthermore, we note that, as the interfaces between layers are smooth, this Sturm-Liouville problem is not singular as it would be in the hypothesis of perfectly sharp interfaces. In this last case the popular method using the partial plane waves of each layer together with continuity conditions at each interface would be more appropriate.

It is well known that the spectrum of SH long-wavelength acoustic phonons in a semi-infinite (in our case, when the slab thickness h goes to infinity) layered medium is the union of a discrete and a continuous part.[1] The latter starts at the transverse threshold of the substrate $\omega_t = c_t q_{||}$, where c_t is the shear horizontal sound velocity of the substrate in the corresponding propagation direction. In the continuous part of the spectrum ($\omega \geqslant \omega_t$), the partial waves of the semi-infinite substrate must be nondecaying bulk waves with real perpendicular wave vectors $q_\perp = (\omega^2/c_t^2 - q_{||}^2)^{1/2}$. Thus only the discrete eigenvalues ($\omega < \omega_t$) correspond to true surface modes or Love waves (*bounded states*) with purely imaginary $q_\perp = i(\omega^2/c_t^2 - q_{||}^2)^{1/2}$, and so exponentially decaying in the substrate. Yet also in the continuous spectrum important structures of surface character (pseudo-Love waves or quasiresonances) can be found.[3,4] With the slab approximation all the phonon spectrum is discrete but shows up as quasi-continuous beyond the transverse threshold of the substrate provided the slab is thick enough. It is then possible to compute the density of phonon states numerically and to simulate the true continuous spectrum of a semi-infinite medium.

We find the whole spectrum of eigenvalues and the corresponding eigenfunctions using the NAG (Ref. 13) routine D02KEF based on a Prufer transformation and a shooting method of integration. In the following, as the most important spectral features are in the low energy part of the spectrum, we use the first 200 eigenvalues with a slab thickness such that the corresponding spectral resolution is better than 200 MHz, in agreement with typical Brillouin measurements.[3,4] In the case of backscattering spectra taken at an incidence angle of 60° the maximum eigenvalue we computed corresponds to approximately 20.5 GHz [see Fig. 3(b)].

The layer-projected phonon density of states LPPDS for the SH polarization[9] is the tool we used to carefully investigate the surface character of the found phonon modes.

The LPPDS can be written as

$$g_{yy}(\omega, q_{||}|z, z')$$

$$= \sum_\alpha \sqrt{\rho(z)\rho(z')} \phi_y(\omega_\alpha(q_{||}), q_{||}, z)$$

$$\times \phi_y(\omega_\alpha(q_{||}), q_{||}, z') \delta[\omega - \omega_\alpha(q_{||})] \qquad (7)$$

and, when computed for $z = z'$,

$$g_{yy}(\omega, q_{||}|z, z) = \sum_\alpha \rho(z) \phi_y^2(\omega_\alpha(q_{||}), q_{||}, z) \delta[\omega - \omega_\alpha(q_{||})]. \qquad (8)$$

For Brillouin light scattering $g_{yy}(\omega, q_{||}|z, z')$ is not simply related to the cross section[4] by a double space integration as it is instead in the case for, e.g., low energy electron surface scattering;[9] the LPPDS is, however, useful to understand both the z (surface) localization and the frequency localization of the phonon modes. If we consider the spectral expansion of the retarded and advanced Green functions of Eq. 4 $G_{yy}(\omega \mp i\epsilon, q_{||}; z, z')$ as the solutions of the nonhomogeneous equation

$$\frac{d}{dz} \left[C_{44}(z) \frac{dG_{yy}}{dz} \right] + [\rho(z)(\omega \mp i\epsilon)^2 - C_{44}(z) q_{||}^2] G_{yy}$$

$$= \delta(z - z') \qquad (9)$$

with the same boundary conditions holding for the ϕ_y's, we obtain a smooth version $\bar{g}_{yy}(\omega, q_{||}|z, z)$ of the LPPDS for SH phonons as

$$\bar{g}_{yy}(\omega, q_{||}|z, z) = \frac{\rho(z)}{2\pi i} [G_{yy}(\omega - i\epsilon, q_{||}; z, z)$$

$$- G_{yy}(\omega + i\epsilon, q_{||}; z, z)], \qquad (10)$$

where ϵ is an infinitesimal real quantity that can be adjusted to simulate a finite experimental spectral resolution.

Once the eigenfrequencies and the corresponding eigenfunctions have been computed, the Green functions can be calculated by means of the spectral expansion[11]

$$G_{yy}(\omega \mp i\epsilon, q_{||}; z, z) = \sum_\alpha \frac{\phi_y^2(\omega_\alpha(q_{||}), q_{||}, z)}{(\omega \mp i\epsilon)^2 - \omega_\alpha^2(q_{||})}. \qquad (11)$$

In the special case of SIMOX structures with sharp interfaces (see below), the analysis of contour plots of the LPPDS put into evidence the surface character of a Brillouin peak, in the continuous part of the spectrum, associated with scattering from pseudo-Love waves.[3,4]

III. TRANSMITTED AND SCATTERED ELECTROMAGNETIC FIELDS

Basically two inelastic light scattering mechanisms are active near the surface of a material: the corrugation (ripple) and the elasto-optic effect.[14] Yet, if we consider only SH waves in [100] and [110] propagation directions of a cubic crystal, the saggital motion is found to be decoupled from the SH one and if, furthermore, we study *p-s* scattering, the ripple contribution is absent for the SH u_y motion and does

not contribute to the vertical displacement of the surface.[4] Thus we consider only the elasto-optic effect. Should not thermal fluctuations be considered, cubic media (like silicon) would have isotropic dielectric properties. Long-wavelength acoustic phonons do cause a variation of the dielectric properties of the medium that can be accounted for by means of an instantaneous anisotropic susceptibility, a second-order random tensor field the components of which are linear functions of the fluctuating elastic strains. Because of dispersion, a simple relation between the polarization vector $\mathbf{P}$ and the electric field can be written only for monochromatic components. We assume that the electric field incident from the vacuum onto the superior surface of the structure is that of a monochromatic plane p wave $(E_x, 0, E_z)$ with circular frequency ω_0 and consider at first the presence of only one SH phonon mode $(\omega(q_{||}), q_{||})$.

The scattered electric field can be computed by first-order perturbation theory because of the smallness of the thermal elastic strains produced in the medium by the phonon excitations.[15]

Neglecting fluctuations at zeroth order, it is convenient to compute first the y component of the magnetic induction field $B_y^{\omega_0}(x, z) = e^{i(k_{||}x)} B(z)$ of the incident p wave transmitted in the medium at depth z and with parallel wave vector $k_{||} = (2\pi/\lambda) \sin\theta_i = (\omega_0/c) \sin\theta_i$. In fact Maxwell's equations for p waves reduce to a single ordinary differential equation for $B(z)$:[12]

$$\frac{d}{dz}\left(\frac{1}{\epsilon(z)}\frac{dB}{dz}\right) + \left(\frac{\omega_0^2}{c^2} - \frac{k_{||}^2}{\epsilon(z)}\right)B = 0. \qquad (12)$$

$\epsilon(z)$ is the z profile of the complex dielectric function of the structure at frequency ω_0.

In the vacuum ($z < 0$), above the surface, $B(z) = (E_0/c)(e^{i(k_\perp z)} - r_p e^{-i(k_\perp z)})$, where E_0 is the electric field amplitude of the incident p wave, $k_\perp = (\omega_0/c)\cos\theta_i$ the component perpendicular to the surface of the wave vector of the incident wave in the vacuum, and r_p the reflection coefficient. Assuming that the substrate is absorbing, we also impose that $B(z)$ vanish as $z \to \infty$.

Following Lekner,[12] we define $q_2(z)$ as the component perpendicular to the surface of the wave vector of the transmitted field in the medium and, writing $\epsilon(z) = \epsilon_r(z) + i\epsilon_i(z)$, the real and imaginary parts of $q_2(z)$ are found from

$$q_2^2(z) = \epsilon(z)\frac{\omega_0^2}{c^2} - k_{||}^2 = \frac{\omega_0^2}{c^2}[\epsilon_r(z) + i\epsilon_i(z) - \sin^2(\theta_i)]. \qquad (13)$$

In the case of a homogeneous medium the dielectric function has just one step at $z = 0$, passing from its vacuum value $\epsilon = 1$ to a constant value $\epsilon > 1$. In this case integration of Eq. (12) gives us a simple plane wave and, imposing that $B(z)$ and $\epsilon^{-1}(z)(dB/dz)$ are continuous at $z = 0$, we find the reflection coefficient as

$$-r_p = \frac{Q_1 - Q_2(0)}{Q_1 + Q_2(0)} = \frac{Q_1 - Q_r(0) - iQ_i(0)}{Q_1 + Q_r(0) + iQ_i(0)}, \qquad (14)$$

where $Q_1 = k_\perp$ and $Q_2(z) = q_2(z)/\epsilon(z)$ are the reduced perpendicular components of the wave vectors. The latter is the ratio of the two complex quantities $q_r(z) + iq_i(z)$ and $\epsilon_r(z) + i\epsilon_i(z)$ with real and imaginary part:

$$Q_r(z) = \frac{\epsilon_r(z)q_r(z) + \epsilon_i(z)q_i(z)}{\epsilon_r^2(z) + \epsilon_i^2(z)}, \qquad (15)$$

$$Q_i(z) = \frac{\epsilon_r(z)q_i(z) - \epsilon_i(z)q_r(z)}{\epsilon_r^2(z) + \epsilon_i^2(z)}. \qquad (16)$$

r_p is a functional of the whole field $B(z)$ and must be computed self-consistently together with it.

Equation (12) can now be rewritten as

$$\frac{d^2B}{dz^2} + \epsilon(z)\left[\frac{d}{dz}\left(\frac{1}{\epsilon(z)}\right)\right]\frac{dB}{dz} + q_2^2(z)B = 0. \qquad (17)$$

We used a numerical method to solve the above equation and obtain both $B(z)$ and r_p. The method was based on the NAG (Ref. 13) FORTRAN routine D02HBF. Because one needs an initial value for r_p to start D02HBF, we obtain such a trial value solving first the problem in the case of a homogeneous semi-infinite medium [see Eqs. (14), (15) and (16)].

Once $B(z)$ has been computed, $E_x^{\omega_0}(x, z)$ and $E_z^{\omega_0}(x, z)$ can be easily obtained as[12]

$$E_x^{\omega_0} = -i\frac{c^2}{\omega_0\epsilon(z)}\frac{\partial B_y^{\omega_0}}{\partial z} = -i\frac{c^2}{\omega_0\epsilon(z)}\frac{dB}{dz}e^{i(k_{||}x)}, \quad (18)$$

$$E_z^{\omega_0} = i\frac{c^2}{\omega_0\epsilon(z)}\frac{\partial B_y^{\omega_0}}{\partial x} = -\frac{c^2 k_{||}}{\omega_0\epsilon(z)}B(z)e^{i(k_{||}x)}. \quad (19)$$

In these last equations the time dependence of all zeroth-order fields has been omitted and is $e^{-i\omega_0 t}$.

The next step is to compute the fluctuating part of the polarization vector in the medium. The first-order result in perturbation theory is

$$P_i^{\omega_s} = \epsilon_0[\epsilon(z) - 1]E_i^{\omega_s} + \epsilon_0\delta\chi_{ij}(\omega_0, \pm\omega_\alpha(q_{||}))E_j^{\omega_0}, \qquad (20)$$

where $\epsilon(z) - 1 = \chi(z)$ is the unperturbed isotropic susceptibility in the absence of the phononic field [because $\omega_\alpha(q_{||}) \ll \omega_0$, we can write $\epsilon(z, \omega_0 \pm \omega_\alpha(q_{||})) \approx \epsilon(z, \omega_0) = \epsilon(z)$] and $\delta\chi_{ij}(\omega_0, \pm\omega_\alpha(q_{||}))$ is the anisotropic fluctuating part of the susceptibility due to the excitation of a single SH $(\omega_\alpha(q_{||}), q_{||})$ phonon mode. The second term on the right hand side of Eq. (20) is responsible for the radiation of the Brillouin light, that is, for the scattered field $\mathbf{E}^{\omega_s}$ at frequencies $\omega_s = \omega_0 \pm \omega_\alpha(q_{||})$.

For p-s scattering it turns out that the fluctuating polarization vector radiating the scattered field has a single component $(P_y^{\omega_s})_R$ which is written as a function of the fluctuating thermal elastic strains $u_{yx} = (1/2)[\partial u_y(\omega_\alpha, q_{||})/\partial x]$ and $u_{yz} = (1/2)[\partial u_y(\omega_\alpha, q_{||})/\partial z]$ as[4]

$$(P_y^{\omega_s})_R = \epsilon_0 k_{44}(z)[u_{yx}(\omega_\alpha, q_{||})E_x^{\omega_0} + u_{yz}(\omega_\alpha, q_{||})E_z^{\omega_0}] \qquad (21)$$

for $[100]$ and as
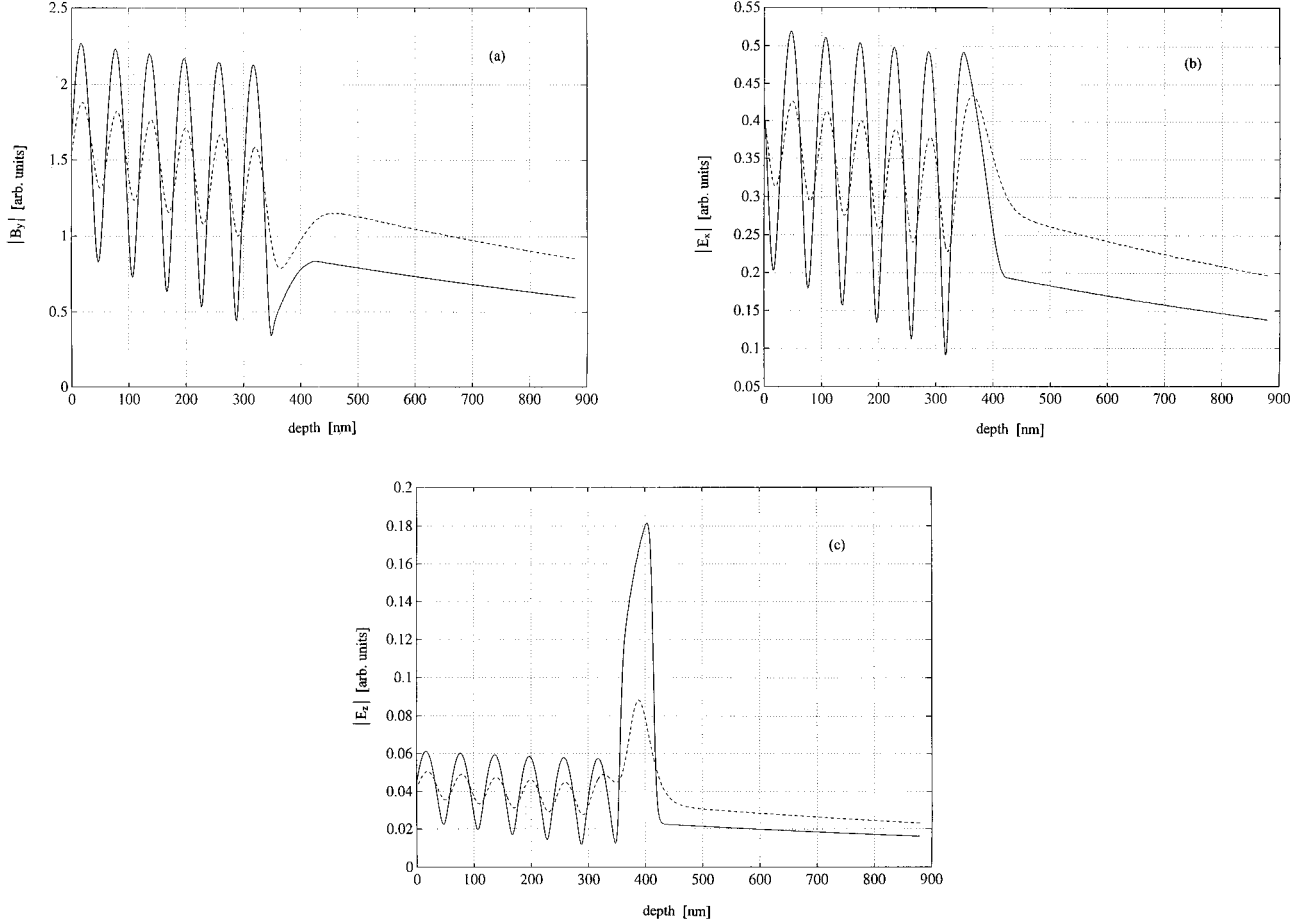
FIG. 2. Zeroth-order transmitted field intensities vs z at $\theta_i = 30°$: $\delta = 1$ nm (solid line), $\delta = 40$ nm (dashed line). (a) Mean square magnetic field B_y; (b) mean square electric field E_x; (c) mean square electric field E_z.

$$(P_y^{\omega_s})_R = \epsilon_0 \{ \tfrac{1}{2} [k_{11}(z) - k_{12}(z)] u_{yx}(\omega_\alpha, q_{||}) E_x^{\omega_0}$$

$$+ k_{44}(z) u_{yz}(\omega_\alpha, q_{||}) E_z^{\omega_0} \} \tag{22}$$

for [110]; the $k_{ij}(z)$ are the z profiles of the elasto-optic coefficients. We notice that Brillouin scattering of an incident p electromagnetic wave off a pure SH phonon produces a scattered s electromagnetic wave, that is, scattering rotates the polarization of 90°.

$(P_y^{\omega_s})_R$ can then be written in the compact form [to save space we write only the anti-Stokes term, radiating at the circular frequency $\omega_s = \omega_0 + \omega_\alpha(q_{||})$, corresponding to the annihilation of pre-existing phonons of the mode α]

$$(P_y^{\omega_s})_R = \xi(\omega_\alpha, q_{||}) \Pi_y(z|\omega_0, k_{||}; \omega_\alpha, q_{||}) e^{i(k_{||} + q_{||})x}. \tag{23}$$

$$\Pi_y(z|\omega_0, k_{||}; \omega_\alpha, q_{||})$$

$$= \frac{c^2 \epsilon_0 k_{44}(z)}{2\omega_0 \epsilon(z)} \left[q_{||} \phi_y(\omega_\alpha(q_{||}), q_{||}, z) \frac{dB}{dz} \right.$$

$$\left. - k_{||} \frac{d\phi_y(\omega_\alpha(q_{||}), q_{||}, z)}{dz} B(z) \right] \tag{24}$$

are spectral weights depending on both the phonon mode profiles and the zeroth-order incident electromagnetic field in

the medium. Around thermal equilibrium, the thermal average of $\xi(\omega_\alpha, q_{||})$ is zero and, therefore, the same is of the average of the scattered field amplitude. Thus, the statistical properties of the Brillouin light depend on the mean square value of $\xi(\omega_\alpha, q_{||})$ and on its time autocorrelation function. If there is no free charge $\text{div}\mathbf{E}^{\omega_s} = -\epsilon_0^{-1}\text{div}\mathbf{P}^{\omega_s}$. The inhomogeneous wave equation for the radiation of the scattered field component $E_y^{s\alpha}(x,z,t) = E_y^\alpha(z) e^{i(k_{||}^s x - \omega_s t)}$ in the medium $(z>0)$ is then obtained from Maxwell's equations as

$$\frac{d^2 E_y^\alpha}{dz^2} + \left[\epsilon(z) \frac{\omega_s^2}{c^2} - k_{||}^{s\,2} \right] E_y^\alpha$$

$$= - \frac{\omega_s^2}{\epsilon_0 c^2} \xi(\omega_\alpha, q_{||}) \Pi_y(z|\omega_0, k_{||}; \omega_\alpha, q_{||}),$$

$$\tag{25}$$

where $k_{||}^s = k_{||} + q_{||}$ is the rule expressing the conservation of parallel wave vector for an anti-Stokes event. The electric field component $E_y^\alpha(z)$ of the scattered s wave is the solution, in the vacuum, above the surface $(z<0)$, of the homogeneous wave equation obtained equating to zero the rhs of Eq. (25) with $\epsilon(z) = 1$. It takes the plane-wave form $E_y^\alpha(z) = E_y^\alpha(0^-) e^{-ik_\perp^s z}$, where $k_\perp^{s\,2} = \omega_s^2/c^2 - k_{||}^{s\,2}$. To compute, in the far field approximation, the total scattered field in the vacuum at the observation point $\mathbf{r}$ within an infinitesimal
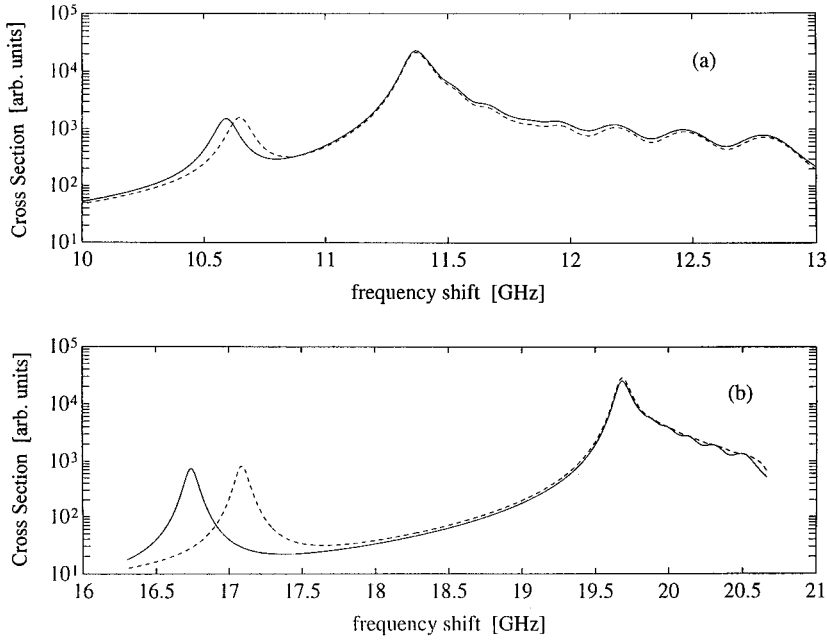
FIG. 3. Theoretical cross section for $\delta = 1$ nm (solid line) and $\delta = 20$ nm (dashed line) for different backscattering geometries: (a) $\theta_i = 30°$; (b) $\theta_i = 60°$.

solid angle $d\Omega$ around the direction of $\mathbf{k}^s = \mathbf{k}_\perp^s + \mathbf{k}_{||}^s$ we are led to calculate $E_y^\alpha(0^-) = E_y^\alpha(0^+) = E_y^\alpha(0)$.

This task can be accomplished by means of numerical integration of Eq. (25), again using the NAG FORTRAN routine D02HBF (Ref. 13) with infinitesimal values of the scattered field and of its z derivative at a depth below the surface much bigger than the skin depth of the substrate.

To obtain the total fluctuating scattered field component $(\omega, \mathbf{k}^s)$, we have to sum up the scattered amplitude at the observation point over all α's, that is, to consider the contribution of all phonon modes having the same parallel wave vector. As a consequence, the differential scattering cross section is proportional, through the factor $S\cos\theta_s$ (S is the illuminated area of the sample surface and θ_s the angle between $\mathbf{k}^s$ and the outgoing surface normal), to the thermal

average of the power spectrum of the total scattered field component, i.e., to the time Fourier transform of its time autocorrelation function.

For the total scattered field we are finally led to the expression

$$E_y^s(\mathbf{r},t) = -\frac{\omega_s^2}{\epsilon_0 c^2} e^{i\mathbf{k}^s\mathbf{r}} \sum_\alpha A_\alpha \xi(\omega_\alpha, q_{||}) e^{i[\omega_0 + \omega_\alpha(q_{||})]t},$$

(26)

where A_α is proportional to $E_y(0)$.

Making use now of the fact that the $\xi(\omega_\alpha, q_{||})$'s are independent random variables with mean square values fixed by the thermal equilibrium conditions $\langle \xi_\alpha^2 \rangle_{\text{th}} = K_B T/S\omega_\alpha^2(q_{||})$,
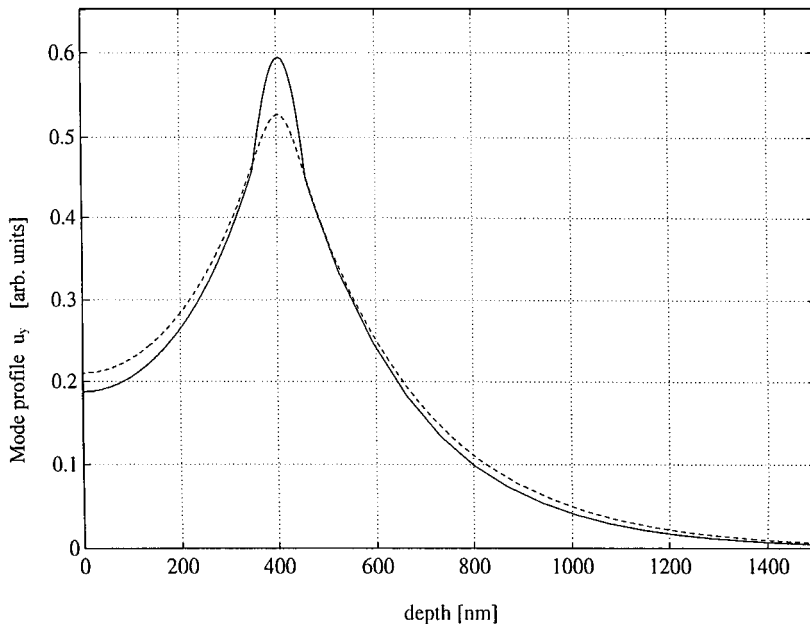
FIG. 4. Mode profiles of Love phonons which would give rise to a Brillouin peak in the discrete part of the spectrum for backscattering with incidence angle $\theta_i = 30°$. $\delta = 1$ nm (solid line) and $\delta = 40$ nm (dashed line).
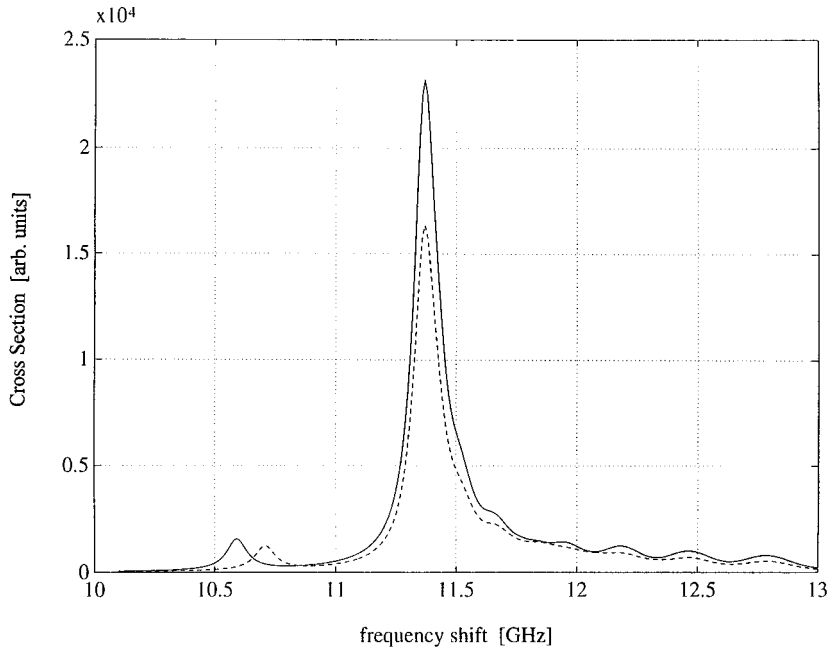
FIG. 5. Theoretical cross section for $\theta_i = 30°$: $\delta = 1$ nm (solid line); $\delta = 40$ nm (dashed line).

we find that the differential scattering cross section for anti-Stokes Brillouin scattering from SH phonons is proportional to

$$\frac{d^2\sigma}{d\Omega d\omega} \propto \cos\theta_s \sum_\alpha \frac{|A_\alpha|^2}{\omega_\alpha^2(q_{||})} \delta\{\omega - [\omega_0 + \omega_\alpha(q_{||})]\}. \quad (27)$$

The Stokes cross section is obtained in a similar way.

IV. A CASE STUDY: IMPERFECT SOI SIMOX STRUCTURES

Recent experimental results on *perfect* SIMOX structures[3,4] motivated us to compute the Brillouin cross sections for scattering from SH acoustic phonons in model im-

perfect structures too. An experimental activity on real imperfect structures is in progress and will be reported elsewhere. For instance, here we treat the case of the presence of silica inclusions in silicon above and below the buried oxyde layer. Figure 1 shows the density profiles of two model SOI SIMOX structures, one with sharp and one with smooth interfaces.

Assuming that the mean inclusion size is much smaller than the typical wavelength of the phonons and photons involved in Brillouin scattering, we are in the Rayleigh scattering regime. Within this approximation the medium can be described by effective constants.[6] Hence our smoothly varying elastic, dielectric, and elasto-optic coefficients can be considered as *local effective constants*.
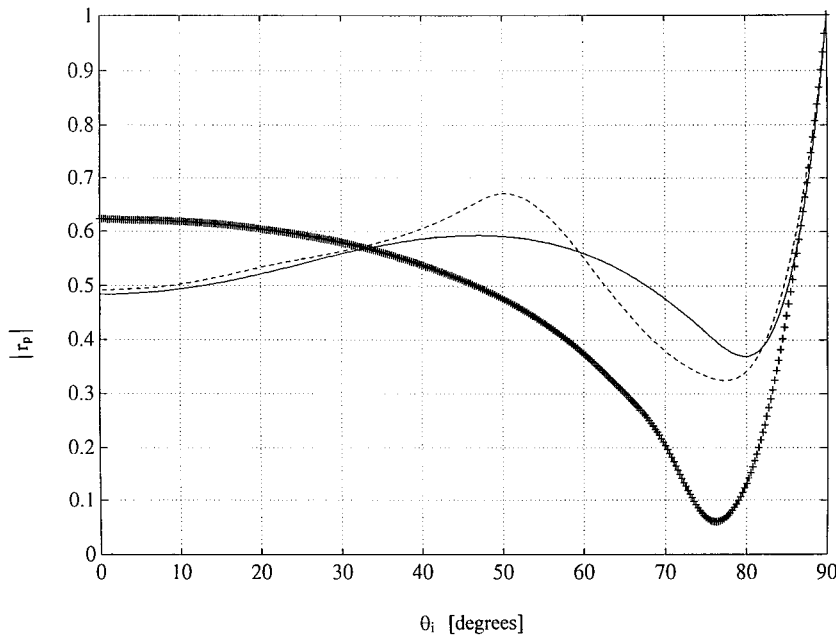
FIG. 6. Modulus of the reflection coefficient r_p vs incidence angle. (+) line, semi-infinite silicon; solid line, SOI structure with $\delta = 5$ nm; dashed line, SOI structure with $\delta = 1$ nm.

The vacuum-Si(001) interface coincides with the $z=0$ plane and the z axis points downwards in the medium. The first Si/SiO$_2$ interface is at $z=d$ and the second SiO$_2$/Si interface is at $z=d+L$. In this application, we assumed that all the functions which describe physical properties of the medium have a local hyperbolic tangent profile. For example, we take a $\rho(z)$ of the form

$$\rho(z) = (\rho_1 - \rho_2)\left\{ 1 - \frac{1}{2}\left[\tanh\left(\frac{z-d_1}{\delta_1}\right) + 1 \right] \right\} + \rho_2$$
$$+ (\rho_1 - \rho_2)\frac{1}{2}\left[\tanh\left(\frac{z-d_2}{\delta_2}\right) + 1 \right], \qquad (28)$$

where (a) ρ_1 and ρ_2 are, respectively, the mass density of Si and SiO$_2$; (b) $d_1=d$, $d_2=d+L$ are, respectively, the first and the second interface depths; and (c) δ_1 and δ_2 characterize the more or less sharpness of the profiles where the properties of the medium change. If $\delta_1 = \delta_2$ we will write δ for both δ_1 and δ_2.

The wavelength of the light incident on the medium is taken as $\lambda_0 = 514.5$ nm. In our computation we used the dielectric (ϵ), elastic (C_{ij}), and elasto-optic constants of bulk Si and SiO$_2$. The Si constants are $\epsilon = 18.5 + 0.52i$, $C_{11} = 166$ GPa, $C_{12} = 63.9$ GPa, $C_{44} = 79.6$ GPa, $K_{11} = 53.2$, $K_{12} = 25.0$, $K_{44} = 23.4$, $\rho = 2330$ k gm^{-3}. The SiO$_2$ constants are $\epsilon = 2.16$, $C_{11} = 78.5$ GPa, $C_{44} = 31.2$ GPa, $K_{11} = -0.55$, $K_{44} = 0.345$, $\rho = 2200$ k gm^{-3}.

Theoretical cross sections are all convoluted with a Lorentzian of 200 MHz width to account for a finite experimental spectral resolution.

Figure 2 shows the depth profiles of the incident transmitted fields at 30° incidence in a SIMOX structure with either $\delta = 1$ nm or $\delta = 40$ nm. One can see that, in the sharper interface case, the surface field intensities are higher than in the smoother case. On the contrary, the penetration depth is higher in the smoother case because the field gradients in the interfacial regions are lower.

In Fig. 3 we illustrate the effect of smooth interfaces on the cross section for p-s Brillouin scattering at two different backscattering angles. As reported in Ref. 3 two peaks associated with scattering off SH phonons exist in the spectrum. The first, below ω_t, is due to the interaction of light with a mode guided in the silica buried layer (a modified Love wave), while the second, beyond ω_t, is to be associated with scattering from a pseudosurface mode, localized mainly in the top silicon layer (a pseudo-Love wave). The principal visible effect is the spectral shift undergone by the low energy peak (Love wave). Repeating this type of computation for several angles, the dispersion laws of both peaks can be obtained.[7]

A comparison between a model structure with sharp and one with smooth interfaces is fully exploited in Figs. 4, 5, and 6. Figure 4 shows the mode profiles [Eq. (4)] corresponding to a Love wave (discrete mode) for these two extreme cases. From a purely acoustic point of view the differences between the two situations are small but visible. One can see that the mode is less localized in the buried oxide layer in the smooth interface case, as one could expect from simple physical considerations. The corresponding phase ve-

locity is higher (see also Fig. 3) because the mode tails propagate in silicon, which has a higher transverse sound speed. It could equally be seen, by a thorough inspection of the LPPDS [Eq. (10)], that the differences in the continuous part of the spectrum are negligible.

In spite of these small differences in the phonon spectrum the cross sections for the two cases look substantially diverse (Fig. 5). Apart from the spectral shift of the first peak (Fig. 4), the main effect is the decrease in the intensity of the peak in the continuum, immediately beyond the transverse threshold. The explanation for the above decrease is to be found in the competition between two antagonist mechanisms. While smooth interfaces tend to allow for a stronger fluctuating polarization in the top silicon they depress (at least with this geometry) the overall back transmission in the vacuum of the scattered light with respect to sharp interfaces. In the chosen example the second phenomenon dominates.

To illustrate the intrinsically self-consistent nature of our method, we also show the computed reflection coefficients. In Fig. 6 the case of semi-infinite silicon is compared with those of two different SIMOX structures with increasingly smooth interfaces. The principal visible effect is the washing out of the pseudo-Brewster angle phenomenon due to interference effects. This last type of information could be correlated with ellipsometry measurements.

V. CONCLUSIONS

We have introduced a method to compute the cross section for Brillouin scattering of light by SH surface acustic phonons in an inhomogeneous medium which is represented by a layered finite slab with arbitrarily smooth interfaces.

The spectra of the acoustic field, the transmitted (zeroth-order), and the scattered (first-order) electromagnetic fields are computed by means of a numerical algorithm which can take into account any depth profile of the physical parameters of the system.

The special case of a model imperfect silicon on insulator structure, with a distribution of silica inclusions in the near-interface regions, is analyzed, putting in evidence the differences between the case with effective sharp interfaces and that with effective smooth interfaces.

We notice that, in different physical situations, the continuous depth profiles would correspond to real diffuse interfaces down to the atomic scale. This is the case of GaAs/Al$_x$Ga$_{1-x}$As superlattices or other real *phononic crystals*[16] for which the application of our method does not require any effective medium approximation but implies the consideration of scattering from longitudinal modes too. Work on normal incidence Brillouin scattering from longitudinal acoustic bulk phonons in imperfect superlattices, following similar guidelines, is in progress and will be published elsewhere.

We wish to stress that only experimental results can allow one to decide which are the more appropriate depth profiles for a given structure; in particular, the theoretical electromagnetic fields can be strongly affected by the specific profiles.

Nevertheless, we emphasize the generality of our method, which is limited only by the requirement of a unidimensional (z) inhomogeneity of the scattering body.

[*]Also at Istituto Nazionale per la Fisica della Materia, Unità di Ricerca Milano Politecnico, Via Ponzio, 34/3 20133 Milano, Italy.

[1]F. Nizzoli and J. R. Sandercock, in *Dynamical Properties of Solids*, edited by G. K. Horton and A. A. Maradudin (Elsevier, Amsterdam, 1990), p. 281.

[2]P. Malischewsky, *Surface Waves and Discontinuities* (Elsevier, Amsterdam, 1987)

[3]C. E. Bottani, G. Ghislotti, and P. Mutti, J. Phys. Condens. Matter **6**, L85 (1994).

[4]G. Ghislotti and C. E. Bottani, Phys. Rev. B **50**, 12 131 (1994).

[5]A. Gagliardi, Thesis, Politecnico di Milano (1995).

[6]G. Grimvall, *Thermophysical Properties of Materials* (North-Holland, Amsterdam, 1986), Chaps. 13 and 14.

[7]C. E. Bottani and R. Caporali, J. Phys. Condens. Matter **6**, L791 (1994).

[8]B. A. Auld, *Acoustic Waves and Fields in Solids Vols. I and II* (Wiley, New York, 1973).

[9]D. L. Mills, S. Y. Tong, and J. E. Black, in *Surface Phonons*, edited by W. Kress and F. W. de Wette (Springer Verlag, Berlin, 1991), p. 200.

[10]H. Sagan, *Boundary and Eigenvalue Problems in Mathematical Physics* (Dover Publications, New York, 1989), p. 163.

[11]R. Courant and D. Hilbert, *Methods of Mathematical Physics Vol. I* (Interscience Publisher, New York, 1953), p. 324.

[12]J. Lekner, *Theory of Reflection* (Martinus Nijhoff Publishers, Dordrecht, 1987), pp. 5 and 157.

[13]Numerical Algorythms Group, NAG Fortran Library Manual, Mark 10 v. 2 (1983)

[14]A. Marvin, V. Bortolani, F. Nizzoli, and G. Santoro, J. Phys. C **13**, 1607 (1980).

[15]V. Bortolani, F. Nizzoli, G. Santoro, and J. R. Sandercock, Phys. Rev. B **25**, 3442 (1982).

[16]M. S. Kushwaha, P. Halevi, G. Martinez, L. Dobrzynski, and B. Djafari-Rouhani, Phys. Rev. B **49**, 2313 (1994).